Published in final edited form as:
Nat Chem Biol. 2010 August ; 6(8): 610–614. doi:10.1038/nchembio.405.

Palmitoylome profiling reveals S-palmitoylation–dependent antiviral activity of IFITM3

Jacob S Yount[1], **Bruno Moltedo**[2], **Yu-Ying Yang**[1], **Guillaume Charron**[1], **Thomas M Moran**[2], **Carolina B López**[2], and **Howard C Hang**[1,*]

[1] The Laboratory of Chemical Biology and Microbial Pathogenesis, The Rockefeller University, New York, New York, USA

[2] Department of Microbiology, The Mount Sinai School of Medicine, New York, New York, USA

Abstract

Identification of immune effectors and the post-translational modifications that control their activity is essential for dissecting mechanisms of immunity. Here we demonstrate that the antiviral activity of interferon-induced transmembrane protein 3 (IFITM3) is post-translationally regulated by S-palmitoylation. Large-scale profiling of palmitoylated proteins in a dendritic cell line using a chemical reporter strategy revealed over 150 lipid-modified proteins with diverse cellular functions, including innate immunity. We discovered that S-palmitoylation of IFITM3 on membrane-proximal cysteines controls its clustering in membrane compartments and its antiviral activity against influenza virus. The sites of S-palmitoylation are highly conserved among the IFITM family of proteins in vertebrates, which suggests that S-palmitoylation of these immune effectors may be an ancient post-translational modification that is crucial for host resistance to viral infections. The S-palmitoylation and clustering of IFITM3 will be important for elucidating its mechanism of action and for the design of antiviral therapeutics.

Vertebrates have evolved sophisticated innate and adaptive mechanisms of immunity to combat microbial pathogens[1]. In response, viruses and pathogenic bacteria have acquired virulence factors that subvert or disarm host defenses[1]. For example, cellular membranes provide a simple barrier to infection, but viruses such as influenza virus have evolved specific proteins that fuse with membranes to allow viral replication inside host cells[2]. Alternatively, intracellular bacterial pathogens are taken up by phagocytic cells, but they then remodel cellular membranes to prevent their own degradation inside lysosomal compartments[3]. Cellular membranes are key interfaces for host resistance and prime targets for microbial virulence factors. We therefore performed large-scale profiling of palmitoylated proteins in phagocytic cells to identify membrane-associated proteins that contribute to immunity against microbial pathogens. We found that S-palmitoylation of interferon-induced transmembrane protein 3 (IFITM3) enhances its clustering in membranes

*Correspondence and requests for materials should be addressed to H.C.H. hhang@rockefeller.edu.

Author contributions

J.S.Y. conceived the study, designed and performed experiments, interpreted data and co-wrote the manuscript; Y.-Y.Y. and G.C. synthesized reagents for palmitoylome profiling studies; B.M., C.B.L. and T.M.M. provided reagents and expertise on influenza virus infections; H.C.H. conceived the study, designed experiments, interpreted data and co-wrote the manuscript.

Competing financial interests

The authors declare no competing financial interests.

Additional information

Supplementary information is available online at http://www.nature.com/naturechemicalbiology/. Reprints and permissions information is available online at http://npg.nature.com/reprintsandpermissions/.

and antiviral activity against influenza virus. Our results demonstrate that large-scale proteomic studies using chemical reporters of post-translational modifications can reveal unique regulatory mechanisms required for cellular resistance to infection.

Protein S-palmitoylation is a covalent fatty acid modification on cysteine residues that is essential for the proper targeting and function of many membrane-associated proteins[4]. Chemical methods with greater sensitivity than classical radiographic techniques have revealed new roles for palmitoylation[5]. Fatty acid analogs functionalized with azides or alkynes, termed chemical reporters, have enabled sensitive fluorescent detection and large-scale proteomic analysis of fatty-acylated proteins using bioorthogonal ligation methods, such as Cu(I)-catalyzed [3 + 2] azide-alkyne cycloaddition (CuAAC) (Fig. 1a)[5]. Fatty acid chemical reporters[6,7] and acyl-biotin exchange methods[8–11] have revealed a greater diversity of S-palmitoylated proteins in eukaryotic proteomes than was previously appreciated and suggest that many cellular pathways are regulated by protein S-palmitoylation. However, the palmitoylomes of phagocytic cells such as dendritic cells (DCs) have not been evaluated. DCs sense pathogen-associated molecular patterns, upregulate immunomodulatory genes and secrete cytokines to activate innate immune responses[12]. Furthermore, DCs are so-called professional antigen-presenting cells with unique abilities to phagocytose, process and present antigens to T cells[13]. The DC palmitoylome is therefore likely to include membrane-associated factors involved in innate or adaptive immunity to microbes.

RESULTS

Proteomic analysis of palmitoylated proteins in DC2.4 cells

To identify lipid-modified and membrane-associated proteins that may contribute to immune responses to microbial infections, we performed large-scale profiling of fatty-acylated proteins in the mouse DC line DC2.4 (ref. [14]) using the palmitic acid chemical reporter alk-16 (ref. [7]) and CuAAC (Fig. 1a). Alk-16 preferentially targets S-palmitoylated proteins[6,7], whereas shorter alkynyl fatty acids selectively label N-myristoylated proteins[7]. In-gel fluorescence profiling of DC2.4 cell lysates reacted with an azide-functionalized fluorophore (az-rho, Supplementary Fig. 1a)[7] demonstrated that a diverse repertoire of proteins are metabolically labeled by alk-16 (Fig. 1b). Cell lysates were then reacted with an azido-biotin cleavable affinity tag (az-diazo-biotin, Supplementary Fig. 1b)[15] for enrichment of alk-16–labeled proteins with streptavidin beads, selective elution and gel-based proteomic identification by mass spectrometry (Supplementary Fig. 1c). Coomassie blue staining of proteins retrieved with streptavidin beads and sodium dithionite elution demonstrates the specificity of alk-16 and CuAAC labeling methods (Supplementary Fig. 1d). Proteins identified in three independent experimental runs (Supplementary Fig. 1d) were compiled and categorized into high- and medium-confidence lists on the basis of the number of assigned spectra, the fold increase above control samples and the number of experiments in which the protein was identified (Supplementary Tables 1 and 2). We selectively identified 157 proteins by alk-16 labeling as compared to control samples (Fig. 1c), with 60 and 97 proteins assigned to high- and medium-confidence lists, respectively (Supplementary Tables 1 and 2). Of these proteins, 52% of high- and 31% of medium-confidence hits have been reported using large-scale proteomic techniques with acyl-biotin exchange chemistry or chemical reporters in other cell types (Supplementary Tables 1 and 2)[6,9,10]. These proteins include calnexin, G protein subunits, transferrin receptor, N-ras, Lyn and CD9 (Fig. 1c and Supplementary Tables 1 and 2). Western blot analysis of alk-16–labeled and enriched DC2.4 cell lysates confirmed robust and specific recovery of calnexin (Supplementary Fig. 1e), the S-palmitoylated protein with the most alk-16 peptide spectral counts compared to control samples (Fig. 1c). Notably, IFITM3 (ref. [16]) was among the candidate S-palmitoylated proteins associated with cellular responses to microbial infections (Fig. 1c).

IFITM3 S-palmitoylation on membrane-proximal residues

Palmitoylation of IFITM3 was investigated further to confirm the high-confidence recovery of IFITM3 by alk-16 proteomics and to explore the potential role of palmitoylation in innate immunity. (Fig. 1c). IFITM3 is a predicted dual-pass transmembrane protein with four homologs, IFITM1, IFITM2, IFITM5 and IFITM6. These proteins range from 11 to 16 kDa, and homologs are present in diverse vertebrates ranging from humans to zebrafish. IFITM3 is commonly used as a marker for developing germ cells[17], though its functional role is unclear[18]. Interaction of IFITM3 with the tetraspanins CD9 and CD81 was demonstrated in B cells, suggesting that this protein localizes to tetraspanin-enriched microdomains[19]. In addition to appearing in B cells, IFITM3 is also constitutively expressed in bone marrow, macrophages and some non-immune cells[19]. The IFITM3 promoter contains interferon-stimulated response elements that control its upregulation upon exposure to the antiviral cytokine interferon (IFN)-α[20,21]. Indeed, IFITM3 transcripts can be readily detected in unstimulated DC2.4 cells and are upregulated upon IFN-α activation (Fig. 2a). These results are consistent with our proteomic data suggesting that IFITM3 is expressed at basal levels in DC2.4 cells without additional stimulation (Fig. 1c). A report of IFITM1 antiviral activity against vesicular stomatitis virus suggested the IFITM protein family plays a role in cellular resistance to viral infections[22]. Notably, small interfering RNA–based screens of host factors involved in H1N1 influenza virus infection identified IFITM3 as a potent inhibitor of early influenza virus replication as well as of dengue and West Nile viruses[16]. The S-palmitoylation of IFITM3 and its potential roles in cellular resistance to virus infection have not been investigated.

IFITM3 amino acid sequence analysis indicates three transmembrane domain–proximal cysteine residues at positions 71, 72 and 105 as potential sites of S-palmitoylation (Fig. 2b). The membrane topology of IFITM3 depicted in Figure 2b is consistent with antibody staining of tagged N and C termini in nonpermeabilized cells[16] as well as staining of the cytoplasmic domain in permeabilized cells[19]. Alk-16 labeling of HeLa cells transfected with hemagglutinin epitope (HA)–tagged IFITM3 followed by anti-HA immunoprecipitation, CuAAC with az-rho and in-gel fluorescence scanning indicated that IFITM3 is indeed fatty acylated (Fig. 2c). To hydrolyze alk-16–protein thioesters, half of the immunoprecipitated material was treated with neutral hydroxylamine (NH_2OH). The resulting decrease in signal is consistent with S-palmitoylation of IFITM3 (Fig. 2c). The three cysteines present in IFITM3 were mutated singly or in combination to alanine and evaluated for alk-16 labeling. Mutation of cysteines 71 and 72 reduces alk-16 labeling, but dual mutation does not result in complete loss of palmitoylation (Fig. 2d). The Cys105 mutant also shows decreased alk-16 labeling, which is completely lost in the C71A C72A C105A triple mutant (palmΔ) (Fig. 2d). Bioinformatic analysis of available IFITM protein sequences revealed that the S-palmitoylated cysteine residues are present in most vertebrates including humans and zebrafish (Supplementary Fig. 2a). In fact, alk-16 labeling of human IFITM1, IFITM2 and IFITM3 suggests S-palmitoylation occurs on all three of these IFITM isoforms (Supplementary Fig. 2b). These results confirmed our alk-16 proteomic data from DC2.4 cells and demonstrated that IFITM3 is S-palmitoylated at three membrane-proximal cysteine residues.

S-palmitoylation controls clustering of IFITM3

We investigated the influence of S-palmitoylation on IFITM3 expression and distribution in HeLa cells. Immunofluorescence analysis revealed that IFITM3 is distributed into punctate clusters (Fig. 3a), whereas IFITM3-palmΔ showed more diffuse staining (Fig. 3a). Costaining of HA-IFITM3–transfected cells with other cellular markers suggests that IFITM3 localizes to the endoplasmic reticulum (ER) and is excluded from lysosomes, as shown by calreticulin and LAMP-1 staining, respectively (Fig. 3b). IFITM3 was also absent

from early endosomes (EEA1 staining), Golgi (golgin-97 staining) and cholesterol-rich membranes (cholera toxin B staining) (Supplementary Fig. 3a). As IFITM3 has been shown to interact with the tetraspanin CD9 (ref. [19]), we evaluated the distribution of HA-IFITM3 in cells expressing GFP-CD9 (Fig. 3b). IFITM3 partially colocalized with GFP-CD9 (Fig. 3b), another S-palmitoylated transmembrane protein (Supplementary Fig. 4a), in membrane compartments that are largely devoid of LAMP-1 staining (Supplementary Fig. 4b). Although IFITM3-palmΔ has a more diffuse staining pattern (Fig. 3a), in colocalization studies the lack of palmitoylation did not appear to grossly alter its cellular distribution in the ER or other cellular organelles (Supplementary Fig. 5). This suggests that palmitoylation controls clustering of IFITM3 in membranes rather than its trafficking to distinct cellular compartments. In summary, both IFITM3 and IFITM3-palmΔ primarily localize to the ER, where their clustering is controlled by S-palmitoylation.

S-palmitoylation regulates IFITM3 antiviral activity

We then determined whether S-palmitoylation was essential for IFITM3 antiviral activity toward influenza virus (H1N1, PR8 strain). Interestingly, infection experiments with pseudotyped viral particles previously demonstrated that the inhibitory activity of IFITM3 is specific to viral envelope glycoproteins, suggesting IFITM3 inhibits viral entry or internalization[16]. We therefore focused on early stages of influenza virus infection. HeLa cells transfected with HA-IFITM3 showed lower levels of influenza viral nucleoprotein (NP) mRNA expression 6 h after infection compared to vector-transfected cells, as measured by qRT-PCR (Fig. 4a). In contrast, viral NP production was mostly unaffected in cells transfected with HA-IFITM3-palmΔ (Fig. 4a), even though wild-type and palmitoylation-defective IFITM3 constructs were expressed at similar levels (Fig. 4a). To confirm these results, we evaluated influenza virus infection of cells by flow cytometry, measuring the protein levels of both HA-IFITM3 and influenza virus NP. Similar to the qRT-PCR results, cells expressing HA-IFITM3 had limited viral NP production 6 h after infection with influenza virus, whereas HA-IFITM3-palmΔ expression afforded comparable amounts of viral NP levels (upper right quadrant of flow cytometry plots) compared to control and non-transfected cells in the same cell culture (Fig. 4b and Supplementary Fig. 6). The observed antiviral activity of IFITM3 upon overexpression in mammalian cells against influenza virus is comparable to the previously reported decrease in viral HA, M2 and NP and is consistent with the cell-autonomous activity of IFITM proteins that was observed using small interfering RNA knockdown or deletion of IFITM3 (ref. [16]). The antiviral activity of IFITM3 was also not a general effect of S-palmitoylated membrane protein overexpression, as transfection of cells with the tetraspanin CD9 had no significant influence on influenza virus replication compared to controls (Fig. 4b). The S-palmitoylation–dependent antiviral activity of IFITM3 was also observed at higher multiplicity of infection with influenza virus (Supplementary Fig. 7).

We also evaluated S-palmitoylation–dependent IFITM3 antiviral activity in HEK293T cells that are more susceptible to influenza virus infection. In accord with our data in HeLa cells (Fig. 4a,b), HEK293T cells expressing HA-IFITM3 (high) inhibited the influenza virus infection compared to non-transfected cells (low) as judged by flow cytometry analysis of influenza NP expression (Supplementary Fig. 8 and Fig. 4c). This antiviral activity was markedly diminished with the S-palmitoylation–deficient HA-IFITM3 construct and not observed for GFP-CD9 (Supplementary Fig. 8 and Fig. 4c). Similar results were also observed using antibody staining to the NS1 protein, another protein produced by influenza virus (Fig. 4c). Replicate experiments demonstrate that HA-IFITM3 expression in HeLa and HEK293T cells inhibits influenza virus infection approximately two-fold compared to non-transfected cells (Fig. 4c). These results are comparable to the two- to fivefold antiviral activity previously observed using A549 cells transduced with retroviral constructs

expressing human IFITM isoforms[16]. The quantitative differences between our data and those published for A549 cells may be due to mouse and human IFITM isoform differences, location of epitope tags, analysis of different viral proteins, methods of overexpression and/or cell type analyzed. Nonetheless, our data demonstrate that mammalian cells expressing higher levels of IFITM3 are more resistant to influenza infection (Fig. 4). This antiviral activity of IFITM3 is dependent on S-palmitoylation, as mutation of modified cysteine residues to alanine abrogates more than 75% of this inhibitory activity (Fig. 4d). Overall, these results indicate that S-palmitoylation of IFITM3 is crucial for its full activity against influenza virus infection.

DISCUSSION

Palmitoylome profiling has revealed a post-translational mechanism important for host defense against viral infections. We discovered that S-palmitoylation of membrane-proximal cysteines on IFITM3 enhances its clustering in membranes and is crucial for its inhibitory activity toward influenza virus infection. Notably, S-palmitoylation does not appear to influence the protein levels of IFITM3, as judged by western blot, immunofluorescence and flow cytometry analyses (Figs. 2–4). In contrast to other S-palmitoylated transmembrane proteins such as LRP6 (ref. [23]) or the anthrax toxin receptor[24], for IFITM3 S-palmitoylation does not appear to grossly regulate its stability or trafficking but rather induces a clustering effect similar to that observed for tetraspanins[25].

As IFITM3 shows specificity toward viral envelope proteins[16] that are often themselves S-palmitoylated[26–28] and clustered for membrane fusion with host cells[2], S-palmitoylation may therefore be required for a multivalent display of these IFN effectors to block the activity of viral envelope proteins such as influenza virus hemagglutinin. Cysteine residues homologous to the S-palmitoylated residues found in mouse IFITM3 are present in IFITM protein isoforms in most vertebrates from humans to zebrafish, suggesting an evolutionarily conserved function for protein S-palmitoylation in innate immunity against microbial pathogens. In contrast to the phenomenon of viruses co-opting host palmitoylation machinery for infection[26–28], S-palmitoylation of an IFN effector, IFITM3, restricts viral infection of host cells. Specific protein lipidation pathways may therefore be prime targets of microbial immune evasion strategies. The identification of S-palmitoylation–dependent IFITM3 clustering and antiviral activity should help elucidate the mechanism by which this family of IFN effectors inhibits virus replication and thus aid in the design of therapeutics targeted at pathogens such as influenza virus.

METHODS

Cells, virus infections, transfections and flow cytometry

HeLa, HEK293T and DC2.4 cells were grown in DMEM with 10% (v/v) FBS. Cells were transfected using Lipofectamine 2000 (Invitrogen). Influenza A virus A/PR/8/34 (H1N1) was propagated in 9-d embryonated chicken eggs and titrated using MDCK cells. For flow cytometry, cells were fixed with PBS and 3.7% (w/v) paraformaldehyde, permeabilized with PBS and 0.2% (w/v) saponin and blocked with PBS and 2% (v/v) FBS. Cells were then incubated with anti-HA antibody (1/1,000, 16B12, Covance), washed three times and stained with goat anti-mouse antibody conjugated to Alexa-488 (1/1,000, Invitrogen). Viral protein was stained using mouse monoclonal antibodies against viral NP (clone HT103)[29] directly conjugated to Alexa-568 or a mouse monoclonal antibody against viral NS1 (clone 1a7 (ref. [30]), provided by J. Yewdell, US National Institutes of Health) conjugated to Alexa-647. Results were analyzed with FlowJo software.

Metabolic labeling, immunoprecipitations and CuACC

Metabolic labeling of DC2.4 or HeLa cells with alk-16 or DMSO control was performed in DMEM and 2% (v/v) charcoal-filtered FBS. Chemical syntheses of alk-16 (ref. [7]), az-rho[7] and az-diazo-biotin[15] have been reported previously. Alk-16–labeled cells were lysed with 0.1 mM triethanolamine (TEA) buffer containing 1% (w/v) Brij97 and Complete EDTA-free protease inhibitor cocktail at 5× concentration (Roche). We diluted 50 μg of protein from the alk-16–labeled and DMSO-treated samples to 34.5 μl with TEA and 1% (w/v) Brij 97 buffer. We added 10 μl 10% (w/v) SDS in H_2O as well as CuAAC reactants including 1 μl of 5 mM az-rho (100 μM final concentration), 1 μl of freshly prepared 50 mM tris(2-carboxyethyl)phosphine hydrochloride (TCEP) (final concentration 1 mM), 2.5 μl 2 mM tris[(1-benzyl-1*H*-1,2,3-triazol-4-yl)methyl]amine (TBTA) (final concentration 100 μM) and 1 μl 50 mM $CuSO_4{\cdot}5H_2O$ (final concentration 1 mM), for a final volume of 50 μl. CuAAC reactions were allowed to proceed for 1 h at room temperature, and a chloroform-methanol precipitation was performed before SDS-PAGE. For immunoprecipitations, 400 μg of cell lysate was added to 15 μl of anti-HA antibody–conjugated agarose (Sigma) in a total volume of 150 μl and rocked at 4 °C for 1 h. Agarose was washed and resuspended in 44.5 μl 0.1 mM TEA and 4% (w/v) SDS, and CuAAC reactants were added as described above. In-gel fluorescence scanning was performed using a Typhoon 9400 imager (Amersham Biosciences). Western blots for HA-tagged proteins were performed using an anti–HA tag polyclonal rabbit antibody (1/1,000, 631207, Clontech).

For proteomic experiments, 5 mg of protein from DC2.4 cells were used. CuAAC reactants were added at the same concentrations as listed above except az-diazo-biotin was substituted for az-rho. Methanol-precipitated and washed protein pellets were resuspended in 1 ml of 0.1 mM TEA, 4% (w/v) SDS and 10 mM EDTA. Equal protein amounts were diluted 1/3 by volume with TEA and 1% (w/v) Brij97 buffer. We added 100 μl prewashed streptavidin agarose beads (Invitrogen) in TEA and 1% (w/v) Brij97 buffer to each sample. The protein and bead mixtures were incubated for 1 h at room temperature on a nutating mixer. The beads were then washed once with PBS and 0.2% (w/v) SDS, three times with PBS and twice with 250 mM ammonium bicarbonate (ABC). Beads were resuspended in 500 μl 8 M urea, and we added 25 μl 200 mM TCEP and 25 μl 400 mM iodoacetamide for capping of reactive cysteine residues. After 30 min, beads were washed twice with 250 mM ABC. Two elutions of proteins from beads were then performed using 250 μl of 25 mM sodium dithionite in 250 mM ABC containing 0.1% (w/v) SDS. Protein was concentrated using a YM-10 Centricon (Millipore). Samples were then subjected to SDS-PAGE and staining with Coomassie blue. DMSO and alk-16 lanes of the gel were then cut for trypsin digestion and peptide extraction. Extracted peptides were dried and resuspended in H_2O and 0.1% (v/v) trifluoroacetic acid for mass spectrometry.

LC-MS analysis

LC-MS analysis was performed with a Dionex 3000 nano-HPLC coupled to an LTQ-Orbitrap ion trap mass spectrometer (ThermoFisher). Peptides were pressure-loaded onto a custom-made 75-μm–diameter, 15-cm C18 reverse-phase column and separated with a gradient running from 95% buffer A (HPLC water with 0.1% (v/v) formic acid) and 5% buffer B (HPLC-grade CH_3CN with 0.1% (v/v) formic acid) to 55% B over 30 min, next ramping to 95% B over 10 min and holding at 95% (v/v) B for 10 min. One full MS scan (300–2000 MW) was followed by three data-dependent scans of the *n*th most intense ions with dynamic exclusion enabled. Peptides from three independent experiments were identified using SEQUEST version 28 and were searched against the mouse International Protein Index (IPI) protein sequence database v3.45. Scaffold software (Proteome Software) was used to compile data from the three experimental runs.

Microscopy

For determination of IFITM3 localization, transfected HeLa cells were fixed with 3.7% (w/v) paraformaldehyde, permeabilized with 0.2% (w/v) saponin or 1% (v/v) Tween and blocked with 2% (v/v) FBS in PBS. Cells were incubated with individual antibodies for 30 min in sequence starting with mouse anti-HA (1/1,000, 16B12, Covance), then goat anti-mouse antibodies conjugated to rhodamine red (1/1,000, Invitrogen), then rabbit antibodies against specific cellular markers or cholera toxin B conjugated to Alexa-488 (Invitrogen) followed by secondary goat anti-rabbit antibodies conjugated to Alexa-488 (1/1,000, Invitrogen). All antibodies were diluted in PBS and 0.2% (w/v) saponin, except for cholera toxin B staining in which PBS and 1% (v/v) Tween 20 was used in all steps. Antibodies against calreticulin (1/500, ab2907, Abcam), LAMP1 (1/500, ab24170, Abcam), EEA1 (1/100, 2411, Cell Signaling) and golgin-97 (1/100, ab33701, Abcam) were used. Cells were incubated with TOPRO-3 (1/1,000, Invitrogen) as a final step.

Cloning, quantitative PCR and topology diagram

IFITM3 and CD9 DNA sequences were amplified by PCR using cDNA prepared from DC2.4 RNA. PCR primers for IFITM3 and CD9 as well as mutagenesis primers for IFITM3 are listed in Supplementary Table 3. DC2.4 cells were treated with 500 ng ml^{-1} IFN-α2 (eBioscience) for 4 h to determine its effect on IFITM3 expression. Reverse transcription and quantitative PCR were performed using a previously described protocol[31,32]. Primers used for quantitative PCR can be found in Supplementary Table 4. The topology diagram of IFITM3 found in Figure 2b was drawn using TOPO2 transmembrane protein display software (http://www.sacs.ucsf.edu/TOPO2/).

Supplementary Material

Refer to Web version on PubMed Central for supplementary material.

Acknowledgments

J.S.Y. is a postdoctoral fellow of the Irving Institute Fellowship Program of the Cancer Research Institute. Y.-Y.Y. was supported in part by the Anderson Cancer Center postdoctoral fellowship. G.C. acknowledges the Weill-Cornell/Rockefeller/Sloan-Kettering Tri-institutional Program in Chemical Biology. The authors would like to thank A. Li for technical support. T.M.M. is supported by grant AI041111 and C.B.L. is supported by grant AI083284-01, both from the US National Institute of Allergy and Infectious Diseases of the US National Institutes of Health. H.C.H. acknowledges support from The Rockefeller University, Ellison Medical Foundation, Irma T. Hirschl and Monique Weill-Caulier Trust, Lerner Trust and the US National Institute of Drug Abuse of the US National Institutes of Health (1R21DA025751-01).

References

1. Finlay BB, McFadden G. Anti-immunology: evasion of the host immune system by bacterial and viral pathogens. Cell 2006;124:767–782. [PubMed: 16497587]
2. Harrison SC. Viral membrane fusion. Nat Struct Mol Biol 2008;15:690–698. [PubMed: 18596815]
3. Flannagan RS, Cosio G, Grinstein S. Antimicrobial mechanisms of phagocytes and bacterial evasion strategies. Nat Rev Microbiol 2009;7:355–366. [PubMed: 19369951]
4. Linder ME, Deschenes RJ. Palmitoylation: policing protein stability and traffic. Nat Rev Mol Cell Biol 2007;8:74–84. [PubMed: 17183362]
5. Charron G, Wilson J, Hang HC. Chemical tools for understanding protein lipidation in eukaryotes. Curr Opin Chem Biol 2009;13:382–391. [PubMed: 19699139]
6. Martin BR, Cravatt BF. Large-scale profiling of protein palmitoylation in mammalian cells. Nat Methods 2009;6:135–138. [PubMed: 19137006]
7. Charron G, et al. Robust fluorescent detection of protein fatty-acylation with chemical reporters. J Am Chem Soc 2009;131:4967–4975. [PubMed: 19281244]

8. Roth AF, et al. Global analysis of protein palmitoylation in yeast. Cell 2006;125:1003–1013. [PubMed: 16751107]
9. Kang R, et al. Neural palmitoyl-proteomics reveals dynamic synaptic palmitoylation. Nature 2008;456:904–909. [PubMed: 19092927]
10. Yang W, Di Vizio D, Kirchner M, Steen H, Freeman MR. Proteome-scale characterization of human S-acylated proteins in lipid raft-enriched and non-raft membranes. Mol Cell Proteomics 2009;9:54–70. [PubMed: 19801377]
11. Zhang J, et al. Identification of CKAP4/p63 as a major substrate of the palmitoyl acyltransferase DHHC2, a putative tumor suppressor, using a novel proteomics method. Mol Cell Proteomics 2008;7:1378–1388. [PubMed: 18296695]
12. Reis e Sousa C. Dendritic cells in a mature age. Nat Rev Immunol 2006;6:476–483. [PubMed: 16691244]
13. Steinman RM, Banchereau J. Taking dendritic cells into medicine. Nature 2007;449:419–426. [PubMed: 17898760]
14. Shen Z, Reznikoff G, Dranoff G, Rock KL. Cloned dendritic cells can present exogenous antigens on both MHC class I and class II molecules. J Immunol 1997;158:2723–2730. [PubMed: 9058806]
15. Yang YY, Ascano JM, Hang HC. Bioorthogonal chemical reporters for monitoring protein acetylation. J Am Chem Soc 2010;132:3640–3641. [PubMed: 20192265]
16. Brass AL, et al. The IFITM proteins mediate cellular resistance to influenza A H1N1 virus, West Nile virus, and dengue virus. Cell 2009;139:1243–1254. [PubMed: 20064371]
17. Saitou M, Barton SC, Surani MA. A molecular programme for the specification of germ cell fate in mice. Nature 2002;418:293–300. [PubMed: 12124616]
18. Lange UC, et al. Normal germ line establishment in mice carrying a deletion of the Ifitm/Fragilis gene family cluster. Mol Cell Biol 2008;28:4688–4696. [PubMed: 18505827]
19. Smith RA, Young J, Weis JJ, Weis JH. Expression of the mouse fragilis gene products in immune cells and association with receptor signaling complexes. Genes Immun 2006;7:113–121. [PubMed: 16395393]
20. Ni Z, et al. Apical role for BRG1 in cytokine-induced promoter assembly. Proc Natl Acad Sci USA 2005;102:14611–14616. [PubMed: 16195385]
21. Neil SJ, Zang T, Bieniasz PD. Tetherin inhibits retrovirus release and is antagonized by HIV-1 Vpu. Nature 2008;451:425–430. [PubMed: 18200009]
22. Alber D, Staeheli P. Partial inhibition of vesicular stomatitis virus by the interferon-induced human 9–27 protein. J Interferon Cytokine Res 1996;16:375–380. [PubMed: 8727077]
23. Abrami L, Kunz B, Iacovache I, van der Goot FG. Palmitoylation and ubiquitination regulate exit of the Wnt signaling protein LRP6 from the endoplasmic reticulum. Proc Natl Acad Sci USA 2008;105:5384–5389. [PubMed: 18378904]
24. Abrami L, Leppla SH, van der Goot FG. Receptor palmitoylation and ubiquitination regulate anthrax toxin endocytosis. J Cell Biol 2006;172:309–320. [PubMed: 16401723]
25. Hemler ME. Tetraspanin functions and associated microdomains. Nat Rev Mol Cell Biol 2005;6:801–811. [PubMed: 16314869]
26. Schmidt MF, Schlesinger MJ. Fatty acid binding to vesicular stomatitis virus glycoprotein: a new type of post-translational modification of the viral glycoprotein. Cell 1979;17:813–819. [PubMed: 226266]
27. Veit M, Schmidt MF, Rott R. Different palmitoylation of paramyxovirus glycoproteins. Virology 1989;168:173–176. [PubMed: 2535902]
28. Chen BJ, Takeda M, Lamb RA. Influenza virus hemagglutinin (H3 subtype) requires palmitoylation of its cytoplasmic tail for assembly: M1 proteins of two subtypes differ in their ability to support assembly. J Virol 2005;79:13673–13684. [PubMed: 16227287]
29. Moltedo B, et al. Cutting edge: stealth influenza virus replication precedes the initiation of adaptive immunity. J Immunol 2009;183:3569–3573. [PubMed: 19717515]
30. Pichlmair A, et al. RIG-I-mediated antiviral responses to single-stranded RNA bearing 5′-phosphates. Science 2006;314:997–1001. [PubMed: 17038589]

31. Yount JS, Gitlin L, Moran TM, Lopez CB. MDA5 participates in the detection of paramyxovirus infection and is essential for the early activation of dendritic cells in response to Sendai Virus defective interfering particles. J Immunol 2008;180:4910–4918. [PubMed: 18354215]

32. Yount JS, Kraus TA, Horvath CM, Moran TM, Lopez CB. A novel role for viral-defective interfering particles in enhancing dendritic cell maturation. J Immunol 2006;177:4503–4513. [PubMed: 16982887]

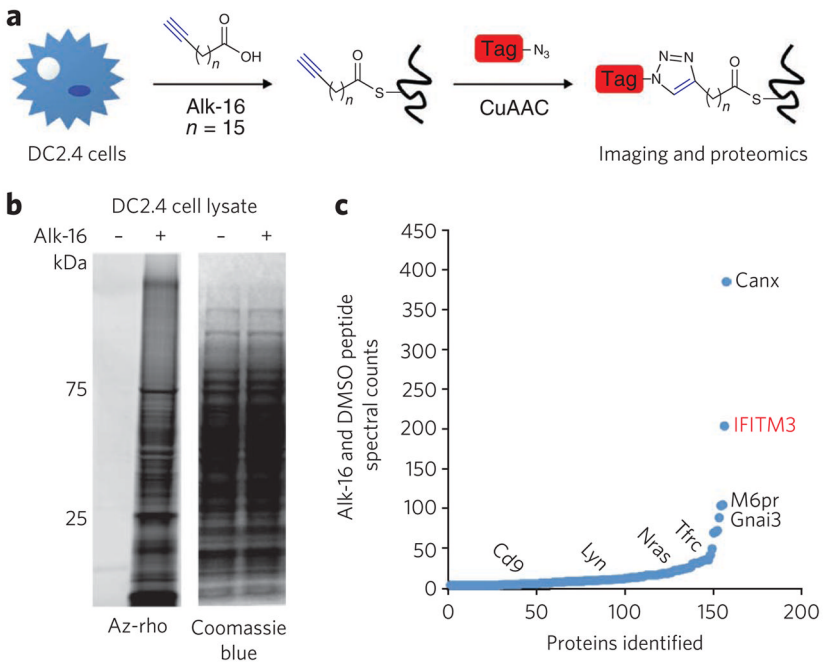

Figure 1. Visualization and identification of palmitoylated proteins in DC2.4 cells

(**a**) Metabolic labeling of cells with alk-16 palmitate reporter and subsequent CuAAC ligation with bioorthogonal detection tags for imaging or proteomics. (**b**,**c**) DC2.4 cells were incubated for 2 h with 50 mM alk-16 or DMSO as a control. In **b**, cell lysates were reacted with az-rho by CuACC, and proteins were separated by SDS-PAGE for visualization by fluorescence gel scanning. Coomassie blue staining demonstrates comparable loading. In **c**, cell lysates were reacted with az-diazo-biotin by CuAAC for enrichment of alk-16–labeled proteins with streptavidin beads and identification by mass spectrometry. For each identified protein, the ratio of peptide spectral counts from the alk-16 and DMSO samples was plotted. Several known palmitoylated proteins are shown in black. IFITM3, the highest-ranked candidate palmitoylated protein, is shown in red.

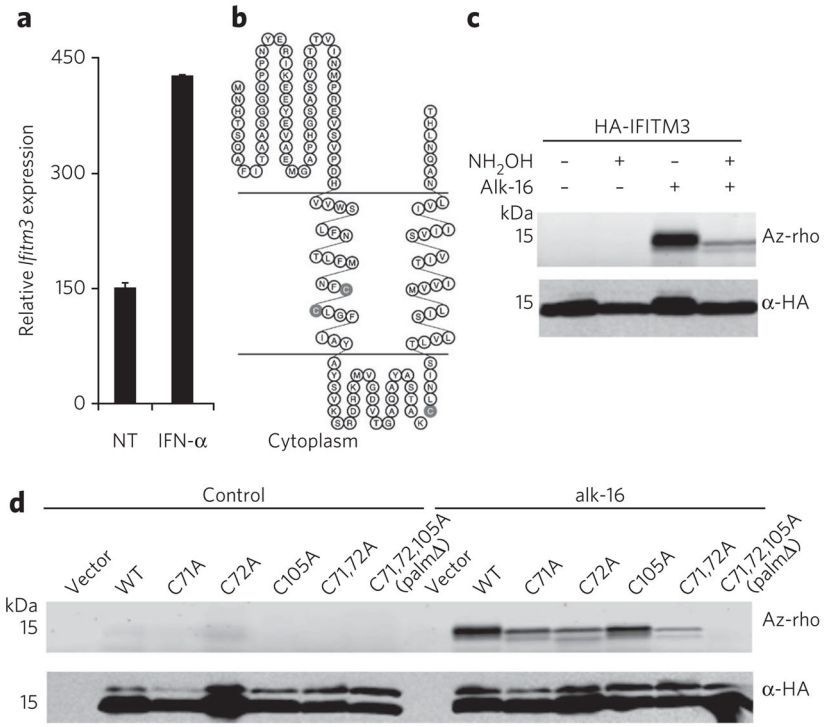

Figure 2. IFITM3 is S-palmitoylated on membrane-proximal cysteine residues

(**a**) *Ifitm3* mRnA expression in DC2.4 cells after 4 h IFn-α treatment as measured by qRt-PCR. NT, non-treated. (**b**) predicted topology of IFITM3 showing the location of cysteine residues (gray shading) with respect to transmembrane domains. (**c**,**d**) HeLa cells were transfected with 2 μg vector, pCMV-HA-IFITM3 wild-type (WT) or cysteine mutants in six-well plates overnight and labeled with 50 μM alk-16 for 2 h. Cell lysates were subjected to anti-HA immunoprecipitation, reacted with az-rho by CuAAC, separated by SDS-PAGE and visualized by fluorescence gel scanning. Comparable protein loading was confirmed by anti-HA western blotting. In **c**, half of the indicated immunoprecipitations were treated with 2.5% (w/v) neutral NH_2OH before boiling and gel loading to hydrolyze protein–alk-16 thioester linkages.

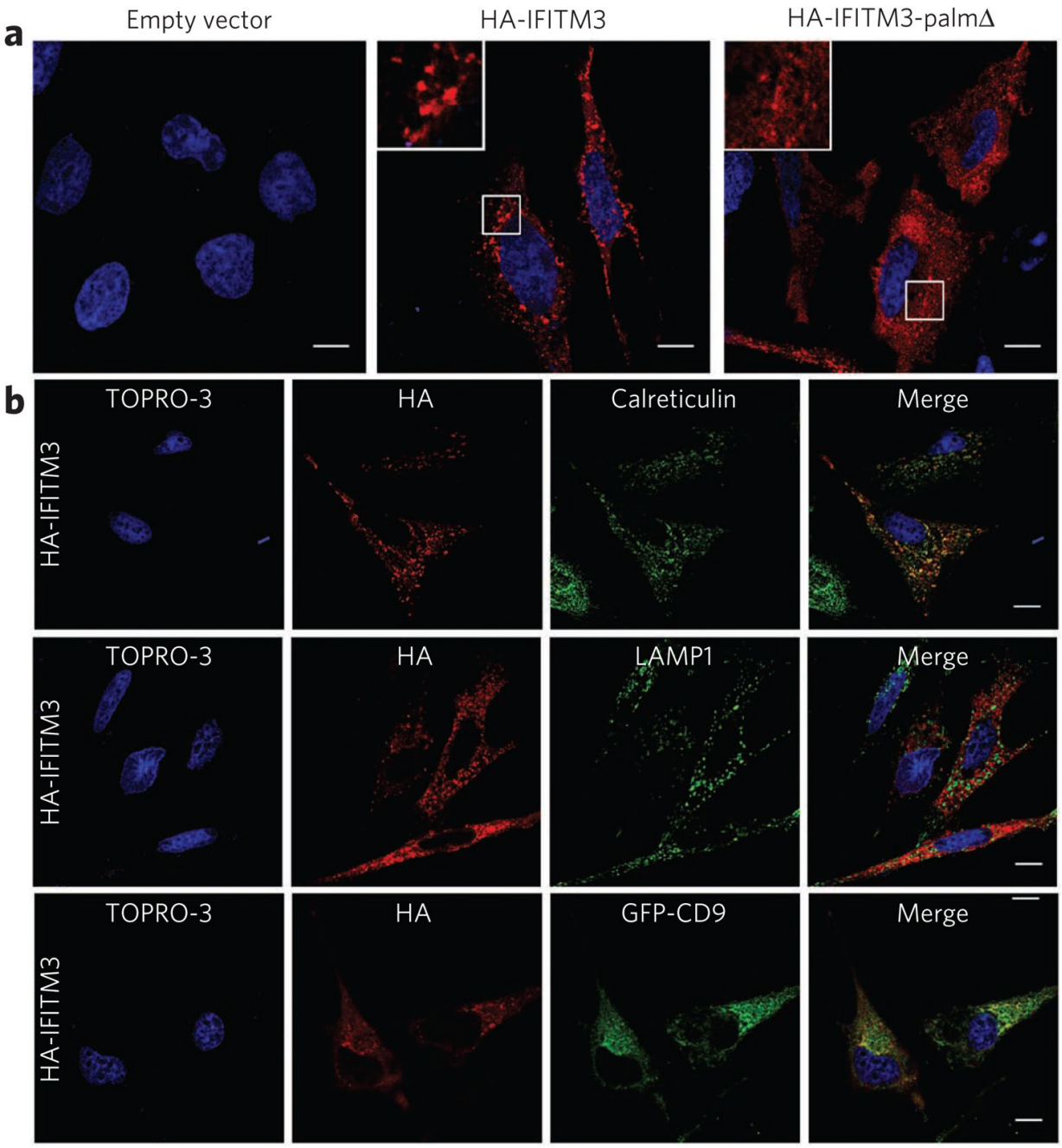

Figure 3. Palmitoylation-dependent clustering of IFITM3 in the ER

(**a**,**b**) HeLa cells grown on coverslips in 12-well plates were transfected with 1 μg pCMV-HA, pCMV-HA-IFITM3 or pCMV-HA-IFITM3-palmΔ and stained with anti-HA (red) and TOPRO-3 (blue). Insets are enlargements of the white-squared regions. Scale bars represent 10 μm. (**b**) Cells were also stained with antibodies against cellular markers, calreticulin and LAMP1 (green), or were co-transfected with GFP-CD9 (green).

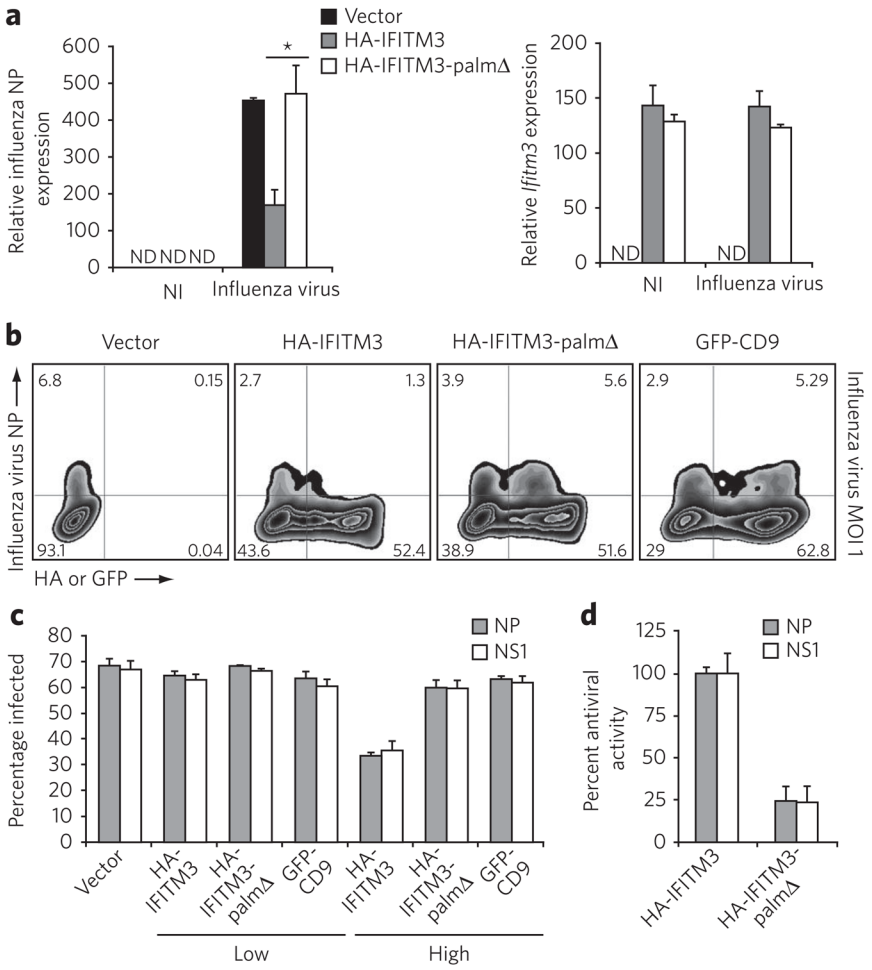

Figure 4. Antiviral activity of IFITM3 is regulated by palmitoylation

(**a**) HeLa cells grown in six-well plates were transfected with 2 μg pCMV-HA, pCMV-HA-IFITM3 or pCMV-HA-IFITM3-palmΔ and infected with influenza virus (PR8 strain) with multiplicity of infection (MOI) of 1 for 6 h. ND, not detected; NI, non-infected. Influenza virus NP mRNA levels and *Ifitm3* expression levels were examined by qRT-PCR. **P* = 0.027 by Student's *t*-test; error represents s.d., *n* = 3. (**b**) HeLa cells grown in 12-well plates were transfected with 1 μg pCMV-HA, pCMV-HA-IFITM3, pCMV-HA-IFITM3-palmΔ or pEGFP-C1-CD9 and infected with influenza virus at an MOI of 1 for 6 h. Virus NP and IFITM3 protein levels were examined by flow cytometry using anti-NP and anti-HA staining, respectively. (**c**) HEK293T cells grown in 12-well plates were transfected with 1 μg pCMV-HA, pCMV-HA-IFITM3, pCMV-HA-IFITM3-palmΔ or pEGFP-C1-CD9 and infected with influenza virus at an MOI of 1 for 6 h. Non-transfected and transfected cells expressing the proteins of interest from the same culture were gated on (labeled "low" and "high," respectively) and analyzed for the percentage of these cells that were infected (Supplementary Fig. 8). Data from flow cytometric analysis of cells staining positive for influenza NP or NS1. (**d**) percentages in **c** were normalized such that the difference in infection rates for vector control and HA-IFITM3 high was set at 100% antiviral activity. Error in **c** and **d** represents s.d., *n* = 4. Note: the HA-tag epitope is derived from an H3 influenza virus strain and is not present in the PR8 strain of H1N1 influenza virus.